Maskless fabrication of plasmonic metasurfaces in polymer film using spatial light modulator

Mohammad H. Bitarafan,*,‡ Shambhavee Annurakshita,‡ Juha Toivonen, Godofredo Bautista

Photonics Laboratory, Physics Unit, Faculty of Engineering and Natural Sciences, Tampere University, Tampere, Finland
**Corresponding author: mohammad.bitarafan@tuni.fi*

‡These authors contributed equally.

Received XX Month XXXX; revised XX Month, XXXX; accepted XX Month XXXX; posted XX Month XXXX (Doc. ID XXXXX); published XX Month XXXX

We demonstrate a high-speed optical technique to fabricate plasmonic metasurfaces in a polymer film. The technique is based on a programmable spatial light modulator, which is used to spatially-control the photoreduction sites of gold ions in a polyvinyl alcohol film doped with a gold precursor. After irradiation, annealing was used to induce the growth of nanoparticles, producing plasmonic microstructures. Using 473 nm excitation wavelength, microscopic plasmonic gratings and meta-atom arrays with arbitrary orientations, an effective nanostructure size of ~700 nm and constituent nanoparticles with average size of ~37 nm were created. The technique enables a cost-effective and straightforward light-based approach to fabricate plasmonic metasurfaces with tunable properties.

Plasmonic metasurfaces are two-dimensional (2D) arrays of subwavelength metal optical resonators that exhibit an unprecedented capability to mold light beyond the reach of conventional planar interfaces, allowing new ways to manipulate light [1,2]. Most experimentally realized metasurfaces have been fabricated based on 'top-down' approaches, including electron-beam lithography [3,4] followed by metal evaporation and focused ion beam milling [5] to ablate already deposited metals. While such techniques provide nanoscale feature sizes, they are expensive and time-consuming and require extreme environments, hindering speed and scalability. Recently, thermal nanoimprint lithography [6] and self-assembly [7] have been used as cost-effective and high-throughput techniques to fabricate metasurfaces, but these involve many fabrication steps hampering flexibility, especially where rapid prototyping is sought.

Light-based methods to create metasurfaces have also been of great interest. Mask-based photolithography has been used to make ultrathin terahertz planar elements [8] and free-form metasurfaces [9]. While this method is popular and appropriate for large-area fabrication, it requires mask preparation and multiprocessing steps. Similarly, interference of two or more beams [10,11] was used to fabricate structures of high structural uniformity and sizes as small as 20 nm [12]. However, the method is limited to 2D nanoparticle (NP) gratings and requires cumbersome implementation. Also, direct laser writing (DLW) [9,13] is used for three-dimensional (3D) manufacturing with sizes approaching 100 nm [14], allowing more complexity in the design. However, DLW relies on serial scanning that is time-consuming, inhibiting speed and scalability. 'Bottom-up' approaches were proposed to simplify the light-based techniques, relying on the exposure of a metal precursor-doped polymer film to laser irradiation to *in situ* photoreduce metal precursors in the polymer film [15–18]. This leads to the formation of spatially organized metal NPs with small feature sizes offering the advantage of single-step syntheses of metal NPs and their assemblies. Such approaches are dependent on cumbersome implementations and are either slow or limited only to periodic structures. Hence, there is a need to develop a high-speed and straightforward method to fabricate plasmonic metasurfaces.

In this Letter, we propose a high-speed technique to fabricate plasmonic metasurfaces in a polymer thin film. The technique is based on a programmable spatial light modulator (SLM) used to spatially control the photoreduction sites of gold ions in a polyvinyl alcohol (PVA) film that is doped with a gold precursor. We use a continuous-wave (CW) laser encoded by an SLM to irradiate the PVA film. Structured light exposure causes *in situ* photoreduction of gold ions at the focal plane. Annealing is performed right after the irradiation to induce further aggregation of gold NPs in the film. This approach significantly simplifies the production of plasmonic metasurfaces within a polymer, enabling low-cost and high-throughput fabrication. Our work opens a new and direct way to rapidly fabricate plasmonic metasurfaces with a complex distribution of meta-atoms.

The overview of the fabrication approach is shown in Fig. 1(a). We used gold (III) chloride trihydrate (Nanopartz, >99.9%) as the gold source and PVA (Sigma-Aldrich, M_w = 89,000-98,000) as the stabilizing agent. These materials were dissolved in distilled water to obtain a 5 wt% polymer solution with a 10% Au/OH ratio. About 1 ml of the resulting solution was spun cast on a borosilicate coverslip at 500 RPM. The samples were kept in a nitrogen desiccator in the dark for 12 hours to ensure that the solvent was completely evaporated, leading to a gold-ion-containing PVA film with ~500 nm thickness.

The optical setup used to fabricate plasmonic structures in PVA film is shown in Fig. 1(b). A CW laser (Cobolt 06-01, 473 nm) was used to illuminate a phase-only Liquid Crystal-on-Silicon (LCOS) SLM (HOLOEYE, HES 6010 BB-HR, 1920 × 1080 resolution, 8 μm pitch, and 87% fill factor) that was calibrated at 473 nm wavelength. A linear polarizer was used to align the incident polarization to the SLM. Another linear polarizer was used after the SLM to further clean the outgoing beam. Specific intensity patterns that mimicked the components of

optical metasurfaces were generated via MATLAB, and subsequently encoded by the SLM to the impinging beam. The phase-encoded beam was passed through relay lenses and a mirror, and then directed towards a microscope objective (LEICA HCX PL APO 100×, oil). The laser power before the objective was set to be adjustable depending on the situation (max of 5 mW). The light distribution at the focal plane of the objective was used to illuminate the PVA film that was mounted on a computer-controlled 3D stage.

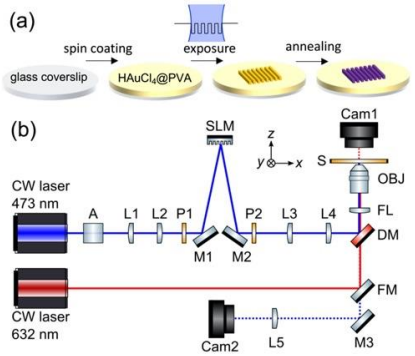

Fig. 1. (a) Scheme of plasmonic grating fabrication in an Au-PVA nanocomposite film using structured light. (b) Scheme of the optical setup used to fabricate metasurfaces and monitor the diffraction from NP gratings. The components include CW lasers (473 and 632 nm), lenses (L1 to L5), attenuator (A), polarizers (P1, P2), mirrors (M1, M2), SLM, flip mirror (FM), flip lens (FL), dichroic mirror (DM), microscope objective (OBJ), stage (S), and cameras (Cam1, Cam2). Respective paths of the incident, reflected, and diffracted light are color-marked.

Upon exposing the film to the incident light, gold ions are reduced into gold atoms [18]. Prolonged exposure leads to the aggregation of gold atoms into larger NPs [19]. Thanks to the light shaping capability of the SLM, the photoreduction sites can be spatially structured at will and in parallel, significantly bypassing the sequential nature of DLW systems for fabricating microscopic entities in polymers [19–21]. Finally, annealing is performed to complete the formation of NPs [18]. Accordingly, the samples were placed on a hot plate with a temperature that was increased progressively to 100 °C within 2 min and kept at 100 °C for an extra 1 min. A CW laser (HeNe, 632 nm) was used to observe the diffraction from the NP gratings (Fig. 1(b)). The beam was guided using a flip mirror, passed through a dichroic mirror, and focused using a lens (200 mm focal length) to the back aperture of an objective (50× LEICA N Plan EPI), leading to a ~10 μm diameter collimated beam. The diffracted light was captured using a CMOS camera. Sample morphology was characterized by a scanning electron microscope (SEM, Zeiss Ultra 55) and an atomic force microscope (AFM, Veeco Dimension 5000, tapping mode). A photodiode power sensor (Ophir, PD300, > 500 pW) was used in the diffraction efficiency measurements.

To investigate the effect of light exposure and dosage on the formation of NPs, we prepared a 150 nm nanocomposite film on a silicon wafer (see Supplement 1). Silicon was chosen to overcome the challenges arising from dielectric films that are deposited on glass in SEM. The film was exposed for 120 sec to a laser beam with 5 mW power modulated via an SLM into 35 μm × 35 μm square regions with known grayscale values, and this irradiated film was subsequently annealed. Figs. 2(a)-(d) show SEM images of an unexposed area of the film, the supposedly dark regions of the intensity pattern or unmodulated parts of the beam, and the desired regions or modulated parts of the beam that correspond to the intentionally exposed areas of the film with ~40 and ~80 W/cm^2 intensities, respectively. As seen in Fig. 2(a), the unexposed area contains some NPs, which were already formed during sample preparation with sizes up to 150 nm. The region associated with the background of the intensity pattern arising from unmodulated light (Fig. 2(b)) shows a significant growth in the number of NPs with sizes between 50-100 nm. The square region that corresponds to the intensity of ~40 W/cm^2 (Fig. 2(c)) indicates a growth in the number of particles with the same range of sizes as in the background (Fig. 2(b)). However, the last region (Fig. 2(d)) exposed to more intense light contains about one order of magnitude more NPs as compared to Fig. 2(c) with an average size of ~37 nm and a standard deviation of ~24 nm (see Supplement 1). These results are in good agreement with a previous report for similar materials exposed to electron-beam, i.e., areas exposed to higher electron-beam doses contained a higher density of smaller NPs [22].

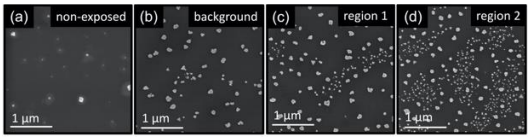

Fig. 2. SEM images from different parts of the Au-PVA film with a thickness of ~150 nm that was (a) unexposed, (b) exposed to the unmodulated beam from the SLM, (c,d) exposed to the modulated beam from the SLM corresponding to (c) ~40 and (d) ~80 W/cm^2 intensities, respectively. The beam power was 5 mW, and the exposure time was 120 sec. The sample was annealed after the exposure.

The ability to manipulate the size and density of NPs in nanocomposite films by merely controlling light intensities prompted us to generate NPs with engineered patterns in the polymer film and study their optical responses. To demonstrate the proof-of-principle of our technique, we fabricated plasmonic diffraction gratings, owing to their simplicity and great importance for applications like bio-sensing [23]. We used the SLM to form microscopic gratings on the polymer film. Figs. 3(a,b) show SEM images corresponding to a small part of an Au-PVA film fabricated by 20-sec exposure to a 3-mW laser beam. Since a 50× objective was used to prepare the samples used in SEM, the exposure was prolonged in order to deliver the same dose of energy as those made on glass via a 100× objective. The grating pattern was designed such that a 3.2 μm pitch was produced at the focal plane. As shown, a high density of NPs was found to exist within the region exposed to the grating pattern. In contrast, the density of NPs was found to be low in the supposedly dark regions. Ultra-thin films with higher gold precursor loads exposed to strong light intensities are expected to lead to higher NP densities.

To demonstrate the flexibility of our technique in fabricating plasmonic gratings of different pitches without the need for mechanical intervention, as seen in traditional interference-based approaches and also in DLW, we fabricated plasmonic gratings with 4, 3.2, 2.8, and 2 μm periodicities in an Au-PVA film. The gratings were made by 5-sec exposure of 30 μm × 30 μm square regions of the film to a 3-mW beam that was guided through the 100× objective. We found that the exposure of light beyond 5 sec had no impact on the structure of the NPs unless the light intensity was high enough to elevate the film temperature. Following the exposure, samples were annealed for 3 min as suggested in Ref. [18]. Large area optical micrographs of the plasmonic gratings fabricated through the exposure to an SLM-structured light are shown in Figs. 3(c)-(f). As seen, there is a clear transmission difference between the grating lines and the background, which is due to the compact

nature of NPs in the exposed regions. A similar experiment on PVA films with no gold loadings has shown no structuring effect (data not shown). This is because the impinging light intensities were not sufficient to drive polymerization at the exposed regions. The intensity images on the right side of each optical micrograph are the diffraction patterns from the corresponding gratings recorded using a HeNe laser (632 nm) beam with ~10 μm diameter at normal incidence. The diffraction efficiency of these structures was measured to be around 1-2%, in good agreement with a previous report [18]. The more compact gratings exhibit more pronounced and resolved diffraction patterns with increased diffraction angles that are consistent with the Bragg's Law of diffraction. The black spot at the central part of the optical micrographs is associated with the zeroth-order of the light coming from the SLM. This spot could be removed by using the spherically and linearly-loaded phase technique [24]. However, given the negligible impact of the over-exposure of the zeroth-order spot, and for the sake of uniformity of the structures, we performed all fabrication experiments such that the bright spot existed at the central part of the patterns.

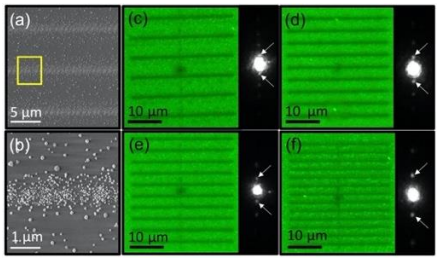

Fig. 3. (a) SEM image of plasmonic gratings fabricated in an Au-PVA film on silicon by 20-sec exposure to a 473 nm structured light with 3-mW power through a 50× objective, and subsequently annealed. (b) A close-up view of the marked region in (a). (c-f) Bright-field optical microscopy images and corresponding diffraction patterns of a HeNe laser (632 nm) from plasmonic gratings with pitches of (c) 4, (d) 3.2, (e) 2.8, and (f) 2 μm fabricated within an Au-PVA film. The samples in (c-f) were fabricated on glass substrates by exposing the films to 3 mW power for 5 sec through 100× objective, and then annealed. The bright spots correspond to zeroth-order, and arrows indicate the first-order mode of the diffraction patterns.

To investigate the effect of light exposure on the surface profile, we acquired an AFM measurement on a grating structure with 3.2 μm pitch, made in an Au-PVA film with a thickness of ~500 nm, exposed to an excitation wavelength of 473 nm with a power of 3 mW through a 100× lens for 5 sec, and annealed as described above. The AFM image is shown in Fig. 4(a). The average surface profile corresponding to Fig. 4(a) is plotted in Fig. 4(b). This line profile suggests that the exposed parts of the sample have raised by ~30 nm, which is in good agreement with the surface relief profile reported in Ref. [18]. Besides, analysis of optical microscopy images of the grating proved that linewidth is linearly proportional to the excitation intensity and exposure time (see Supplement 1). AFM and SEM images (Fig. 3) revealed that the NPs exist both on the surface and within the polymer film. Since the depth-of-field in our setup is greater than the film thickness, we expect NPs to exist in the entire thickness.

The key advantage of our technique, as opposed to interference patterning, is the possibility of making non-uniform patterns of microstructures within the composite film, which is an indispensable requirement for metasurfaces that have applications in beam steering and shaping [25–27]. In the context of nonlinear optics, such distributions of meta-atoms were found to significantly modify the overall second-harmonic generation efficiency of the structures [28]. To prove this possibility, we encoded the SLM with a range of L-shaped patterns and exposed the Au-PVA film for only 5 sec (Fig. 5(a)). In principle, any 1D or 2D arrangement of meta-atoms of arbitrary shape and orientation is feasible due to the versatile light-shaping capability of the SLM. Figure 5(b) shows a bright-field optical microscopy image of the fabricated structure with varied orientations. An AFM image of the same sample is illustrated in Fig. 5(c), which is expected to have similar surface relief modulation as in Fig. 4. NPs are visible in the non-irradiated area formed due to the unmodulated light in the background (as discussed before). Of note, owing to the Au-PVA film's absorption band centered at ~324 nm [17], the photoreduction is remarkably faster at shorter wavelengths [19]. Hence, a light source with a suitable wavelength and sufficient intensity could expedite the above fabrication to occur in the millisecond range, which outperforms state-of-the-art metal DLW with scanning speeds in the range of a few μm/s [29]. This enables quick and straightforward fabrication within the optical setup and without the exclusive need for an expensive lithography and/or cleanroom equipment. Importantly, the technique can be further developed to fabricate prototypes of metasurfaces that support various subwavelength functionalities such as beam shaping, manipulation, and focusing.

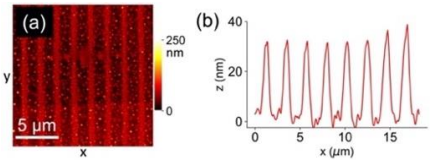

Fig. 4. (a) AFM image of a plasmonic grating made in an Au-PVA film on glass with a thickness of ~500 nm, exposed to an excitation wavelength of 473 nm and power of 3 mW through a 100× lens for 5 sec, and subsequently annealed. (b) Averaged surface profile along *x*-axis corresponding to the AFM image in (a).

The proposed method also has several limitations. For metasurface application, the ability to control the size of NPs and features of meta-atoms are essential. The minimum feature size is always limited by the diffraction of light. Using the present capabilities of our technique, the smallest linewidth was found to be close to 700 nm, implying that these plasmonic metasurfaces could be most useful for long visible to NIR excitations. To reach linewidths suitable for plasmonics research in the visible regime, one could exploit methods that allow the fabrication of sub-diffraction features, e.g., femtosecond lasers via multiphoton absorption [30] or shaped light fields with sub-diffraction transversal confinements [31]. Next, the unmodulated light coming from the SLM leads to the photoreduction of the background film, i.e., the regions hosting the meta-atoms, leading to lower contrast. Therefore, improving the spatial distribution of the modulated light is expected to improve the quality and functionality of the fabricated devices [24,32]. Another possible solution could be developing the exposed film in an appropriate solvent to entirely remove the background, which is somewhat similar to lithographically-made metasurfaces. We also anticipate that our technique can be exploited for other metal precursors (e.g., silver, copper, or aluminum) [33]. However, different light intensities required to photoreduce other metal ions could ablate the film, leading to the creation of grooves instead of bumps in the exposed region [20]. Other polymers (e.g., PMMA) can also be used as

the stabilizing matrix, but with a possible need for additional precursors to absorb light and induce photoreduction. The diffraction efficiency of these structures is about 50% lower than that of similar structures in thicker polymer films [18]. This could be attributed to the smaller film height modulations and smaller AuNP sizes, which cause suboptimal coupling of the incident light. We anticipate that a modified annealing step could fine-tune the plasmon resonance, leading to a higher diffraction efficiency. Finally, we expect that overcoming such limitations would be valuable in extending the technique to fabricate volume elements. In laboratory-scale prototyping, which is already permitted by moderate quality metasurfaces, it would undoubtedly be advantageous to exploit such a cost-effective and straightforward technique and tune fabrication parameters at will. This will be too costly or lengthy to do in traditional fabrication techniques such as an electron-beam lithography or DLW system in tandem with routine sample preparations in the cleanroom.

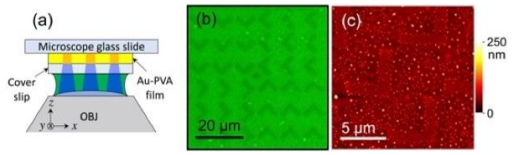

Fig. 5. (a) Scheme of plasmonic metasurface fabrication in an Au-PVA film using structured light. (b) Fabricated arrays of gold NPs in the form of L-shaped structures of varied orientations on a glass coverslip. The pattern was made in an Au-PVA film with a thickness of ~500 nm, through a 5-sec exposure of 473 nm excitation wavelength originating from an SLM. The sample was annealed right after the exposure. The power of the input light was measured to be ~3 mW and was delivered to the sample through a 100× objective. (c) AFM image of the L-shaped structures that were fabricated using the same parameters as in (b).

To conclude, we demonstrated the fabrication of plasmonic metasurfaces in an Au-PVA nanocomposite film using structured light. Meta-atoms as small as ~700 nm containing NPs with an average size of 37 nm were realized. We verified and showed the possibility of fabricating more complex metasurfaces through the same technique and material. This simple and cost-effective approach enables the rapid prototyping of plasmonic metasurfaces with tunable properties. Such metasurfaces could be useful in applications such as beam shaping and manipulation, optical communication, and nonlinear optics.

Funding. Academy of Finland (No. 310801). Academy of Finland Flagship Programme PREIN (No. 320165). S.A. is grateful to Jenny and Antti Wihuri Foundation for financial support.

Acknowledgments. This work made use of the Aalto University Nanomicroscopy Center (Aalto-NMC) premises.

Disclosures. The authors declare no conflicts of interest.

See Supplement 1 for supporting content.

References

1. N. Meinzer, W. L. Barnes, and I. R. Hooper, Nat. Photonics **8**, 889 (2014).
2. H.-H. Hsiao, C. H. Chu, and D. P. Tsai, Small Methods **1**, 1600064 (2017).
3. F. Ding, Y. Chen, Y. Yang, and S. I. Bozhevolnyi, Adv. Opt. Mater. **7**, 1900724 (2019).
4. R. A. Maniyara, D. Rodrigo, R. Yu, J. Canet-Ferrer, D. S. Ghosh, R. Yongsunthon, D. E. Baker, A. Rezikyan, F. J. García de Abajo, and V. Pruneri, Nat. Photonics **13**, 328 (2019).
5. C. Enkrich, F. Pérez-Willard, D. Gerthsen, J. F. Zhou, T. Koschny, C. M. Soukoulis, M. Wegener, and S. Linden, Adv. Mater. **17**, 2547 (2005).
6. W. Chen, M. Tymchenko, P. Gopalan, X. Ye, Y. Wu, M. Zhang, C. B. Murray, A. Alu, and C. R. Kagan, Nano Lett. **15**, 5254 (2015).
7. J. Y. Kim, H. Kim, B. H. Kim, T. Chang, J. Lim, H. M. Jin, J. H. Mun, Y. J. Choi, K. Chung, J. Shin, S. Fan, and S. O. Kim, Nat. Commun. **7**, 12911 (2016).
8. D. Hu, X. Wang, S. Feng, J. Ye, W. Sun, Q. Kan, P. J. Klar, and Y. Zhang, Adv. Opt. Mater. **1**, 186 (2013).
9. J.-H. Yoo, H. T. Nguyen, N. J. Ray, M. A. Johnson, W. A. Steele, J. M. Chesser, S. H. Baxamusa, S. Elhadj, J. T. McKeown, M. J. Matthews, and E. Feigenbaum, ACS Appl. Mater. Interfaces **11**, 22684 (2019).
10. C. Lu and R. H. Lipson, Laser Photonics Rev. **4**, 568 (2010).
11. Z. Zhang, J. Luo, M. Song, and H. Yu, Appl. Phys. Lett. **107**, 241904 (2015).
12. S. R. J. Brueck, Proc. IEEE **93**, 1704 (2005).
13. S. Bagheri, K. Weber, T. Gissibl, T. Weiss, F. Neubrech, and H. Giessen, ACS Photonics **2**, 779 (2015).
14. F. Formanek, N. Takeyasu, T. Tanaka, K. Chiyoda, A. Ishikawa, and S. Kawata, Appl. Phys. Lett. **88**, 083110 (2006).
15. S. Shukla, X. Vidal, E. P. Furlani, M. T. Swihart, K.-T. Kim, Y.-K. Yoon, A. Urbas, and P. N. Prasad, ACS Nano **5**, 1947 (2011).
16. R. P. Chaudhary, G. Ummethala, A. Jaiswal, S. Hawal, S. Saxena, and S. Shukla, RSC Adv. **6**, 113457 (2016).
17. K. Kaneko, H.-B. Sun, X.-M. Duan, and S. Kawata, Appl. Phys. Lett. **83**, 1426 (2003).
18. E. Nadal, N. Barros, H. Glénat, J. Laverdant, D. S. Schmool, and H. Kachkachi, J. Mater. Chem. C **5**, 3553 (2017).
19. M. H. Bitarafan, S. Suomala, and J. Toivonen, Opt. Mater. Express **10**, 138 (2020).
20. P. Kunwar, J. Hassinen, G. Bautista, R. H. A. Ras, and J. Toivonen, ACS Nano **8**, 11165 (2014).
21. N. Karimi, P. Kunwar, J. Hassinen, R. H. A. Ras, and J. Toivonen, Opt. Lett. **41**, 3627 (2016).
22. J. Marqués-Hueso, R. Abargues, J. Canet-Ferrer, S. Agouram, J. L. Valdés, and J. P. Martínez-Pastor, Langmuir **26**, 2825 (2010).
23. W.-H. Yeh, J. W. Petefish, and A. C. Hillier, Anal. Chem. **83**, 6047 (2011).
24. H. Zhang, J. Xie, J. Liu, and Y. Wang, Appl. Opt. **48**, 5834 (2009).
25. N. Yu, P. Genevet, M. A. Kats, F. Aieta, J.-P. Tetienne, F. Capasso, and Z. Gaburro, Science **334**, 333 (2011).
26. L. Huang, X. Chen, H. Mühlenbernd, G. Li, B. Bai, Q. Tan, G. Jin, T. Zentgraf, and S. Zhang, Nano Lett. **12**, 5750 (2012).
27. Z. Liu, Z. Li, Z. Liu, H. Cheng, W. Liu, C. Tang, C. Gu, J. Li, H.-T. Chen, S. Chen, and J. Tian, ACS Photonics **4**, 2061 (2017).
28. H. Husu, R. Siikanen, J. Mäkitalo, J. Lehtolahti, J. Laukkanen, M. Kuittinen, and M. Kauranen, Nano Lett. **12**, 673 (2012).
29. E. H. Waller, S. Dix, J. Gutsche, A. Widera, and G. von Freymann, Micromachines **10**, 827 (2019).
30. G. Bautista, M. J. Romero, G. Tapang, and V. R. Daria, Opt. Commun. **282**, 3746 (2009).
31. L. Turquet, X. Zang, J.-P. Kakko, H. Lipsanen, G. Bautista, and M. Kauranen, Opt. Express **26**, 27572 (2018).
32. A. Jesacher, C. Maurer, A. Schwaighofer, S. Bernet, and M. Ritsch-Marte, Opt. Express **16**, 2597 (2008).
33. P. Kunwar, L. Turquet, J. Hassinen, R. H. A. Ras, J. Toivonen, and G. Bautista, Opt. Mater. Express **6**, 946 (2016).

Full References

1. N. Meinzer, W. L. Barnes, and I. R. Hooper, "Plasmonic meta-atoms and metasurfaces," Nat. Photonics **8**(12), 889–898 (2014).
2. H.-H. Hsiao, C. H. Chu, and D. P. Tsai, "Fundamentals and Applications of Metasurfaces," Small Methods **1**(4), 1600064 (2017).
3. F. Ding, Y. Chen, Y. Yang, and S. I. Bozhevolnyi, "Multifunctional Metamirrors for Broadband Focused Vector-Beam Generation," Adv. Opt. Mater. **7**(22), 1900724 (2019).
4. R. A. Maniyara, D. Rodrigo, R. Yu, J. Canet-Ferrer, D. S. Ghosh, R. Yongsunthon, D. E. Baker, A. Rezikyan, F. J. García de Abajo, and V. Pruneri, "Tunable plasmons in ultrathin metal films," Nat. Photonics **13**(5), 328–333 (2019).
5. C. Enkrich, F. Pérez-Willard, D. Gerthsen, J. F. Zhou, T. Koschny, C. M. Soukoulis, M. Wegener, and S. Linden, "Focused-Ion-Beam Nanofabrication of Near-Infrared Magnetic Metamaterials," Adv. Mater. **17**(21), 2547–2549 (2005).
6. W. Chen, M. Tymchenko, P. Gopalan, X. Ye, Y. Wu, M. Zhang, C. B. Murray, A. Alu, and C. R. Kagan, "Large-Area Nanoimprinted Colloidal Au Nanocrystal-Based Nanoantennas for Ultrathin Polarizing Plasmonic Metasurfaces," Nano Lett. **15**(8), 5254–5260 (2015).
7. J. Y. Kim, H. Kim, B. H. Kim, T. Chang, J. Lim, H. M. Jin, J. H. Mun, Y. J. Choi, K. Chung, J. Shin, S. Fan, and S. O. Kim, "Highly tunable refractive index visible-light metasurface from block copolymer self-assembly," Nat. Commun. **7**(1), 12911 (2016).
8. D. Hu, X. Wang, S. Feng, J. Ye, W. Sun, Q. Kan, P. J. Klar, and Y. Zhang, "Ultrathin Terahertz Planar Elements," Adv. Opt. Mater. **1**(2), 186–191 (2013).
9. J.-H. Yoo, H. T. Nguyen, N. J. Ray, M. A. Johnson, W. A. Steele, J. M. Chesser, S. H. Baxamusa, S. Elhadj, J. T. McKeown, M. J. Matthews, and E. Feigenbaum, "Scalable Light-Printing of Substrate-Engraved Free-Form Metasurfaces," ACS Appl. Mater. Interfaces **11**(25), 22684–22691 (2019).
10. C. Lu and R. H. Lipson, "Interference lithography: a powerful tool for fabricating periodic structures," Laser Photonics Rev. **4**(4), 568–580 (2010).
11. Z. Zhang, J. Luo, M. Song, and H. Yu, "Large-area, broadband and high-efficiency near-infrared linear polarization manipulating metasurface fabricated by orthogonal interference lithography," Appl. Phys. Lett. **107**(24), 241904 (2015).
12. S. R. J. Brueck, "Optical and Interferometric Lithography - Nanotechnology Enablers," Proc. IEEE **93**(10), 1704–1721 (2005).
13. S. Bagheri, K. Weber, T. Gissibl, T. Weiss, F. Neubrech, and H. Giessen, "Fabrication of Square-Centimeter Plasmonic Nanoantenna Arrays by Femtosecond Direct Laser Writing Lithography: Effects of Collective Excitations on SEIRA Enhancement," ACS Photonics **2**(6), 779–786 (2015).
14. F. Formanek, N. Takeyasu, T. Tanaka, K. Chiyoda, A. Ishikawa, and S. Kawata, "Selective electroless plating to fabricate complex three-dimensional metallic micro/nanostructures," Appl. Phys. Lett. **88**(8), 083110 (2006).
15. S. Shukla, X. Vidal, E. P. Furlani, M. T. Swihart, K.-T. Kim, Y.-K. Yoon, A. Urbas, and P. N. Prasad, "Subwavelength Direct Laser Patterning of Conductive Gold Nanostructures by Simultaneous Photopolymerization and Photoreduction," ACS Nano **5**(3), 1947–1957 (2011).
16. R. P. Chaudhary, G. Ummethala, A. Jaiswal, S. Hawal, S. Saxena, and S. Shukla, "One-step, subwavelength patterning of plasmonic gratings in metal–polymer composites," RSC Adv. **6**(114), 113457–113462 (2016).
17. K. Kaneko, H.-B. Sun, X.-M. Duan, and S. Kawata, "Two-photon photoreduction of metallic nanoparticle gratings in a polymer matrix," Appl. Phys. Lett. **83**(7), 1426–1428 (2003).
18. E. Nadal, N. Barros, H. Glénat, J. Laverdant, D. S. Schmool, and H. Kachkachi, "Plasmon-enhanced diffraction in nanoparticle gratings fabricated by in situ photo-reduction of gold chloride doped polymer thin films by laser interference patterning," J. Mater. Chem. C **5**(14), 3553–3560 (2017).
19. M. H. Bitarafan, S. Suomala, and J. Toivonen, "Sub-microwatt direct laser writing of fluorescent gold nanoclusters in polymer films," Opt. Mater. Express **10**(1), 138 (2020).
20. P. Kunwar, J. Hassinen, G. Bautista, R. H. A. Ras, and J. Toivonen, "Direct Laser Writing of Photostable Fluorescent Silver Nanoclusters in Polymer Films," ACS Nano **8**(11), 11165–11171 (2014).
21. N. Karimi, P. Kunwar, J. Hassinen, R. H. A. Ras, and J. Toivonen, "Micropatterning of silver nanoclusters embedded in polyvinyl alcohol films," Opt. Lett. **41**(15), 3627 (2016).
22. J. Marqués-Hueso, R. Abargues, J. Canet-Ferrer, S. Agouram, J. L. Valdés, and J. P. Martínez-Pastor, "Au-PVA Nanocomposite Negative Resist for One-Step Three-Dimensional e-Beam Lithography," Langmuir **26**(4), 2825–2830 (2010).
23. W.-H. Yeh, J. W. Petefish, and A. C. Hillier, "Diffraction-Based Tracking of Surface Plasmon Resonance Enhanced Transmission Through a Gold-Coated Grating," Anal. Chem. **83**(15), 6047–6053 (2011).
24. H. Zhang, J. Xie, J. Liu, and Y. Wang, "Elimination of a zero-order beam induced by a pixelated spatial light modulator for holographic projection," Appl. Opt. **48**(30), 5834 (2009).
25. N. Yu, P. Genevet, M. A. Kats, F. Aieta, J.-P. Tetienne, F. Capasso, and Z. Gaburro, "Light Propagation with Phase Discontinuities: Generalized Laws of Reflection and Refraction," Science **334**(6054), 333–337 (2011).
26. L. Huang, X. Chen, H. Mühlenbernd, G. Li, B. Bai, Q. Tan, G. Jin, T. Zentgraf, and S. Zhang, "Dispersionless Phase Discontinuities for Controlling Light Propagation," Nano Lett. **12**(11), 5750–5755 (2012).
27. Z. Liu, Z. Li, Z. Liu, H. Cheng, W. Liu, C. Tang, C. Gu, J. Li, H.-T. Chen, S. Chen, and J. Tian, "Single-Layer Plasmonic Metasurface Half-Wave Plates with Wavelength-Independent Polarization Conversion Angle," ACS Photonics **4**(8), 2061–2069 (2017).
28. H. Husu, R. Siikanen, J. Mäkitalo, J. Lehtolahti, J. Laukkanen, M. Kuittinen, and M. Kauranen, "Metamaterials with Tailored Nonlinear Optical Response," Nano Lett. **12**(2), 673–677 (2012).
29. E. H. Waller, S. Dix, J. Gutsche, A. Widera, and G. von Freymann, "Functional Metallic Microcomponents via Liquid-Phase Multiphoton Direct Laser Writing: A Review," Micromachines **10**(12), 827 (2019).
30. G. Bautista, M. J. Romero, G. Tapang, and V. R. Daria, "Parallel two-photon photopolymerization of microgear patterns," Opt. Commun. **282**(18), 3746–3750 (2009).
31. L. Turquet, X. Zang, J.-P. Kakko, H. Lipsanen, G. Bautista, and M. Kauranen, "Demonstration of longitudinally polarized optical needles," Opt. Express **26**(21), 27572 (2018).
32. A. Jesacher, C. Maurer, A. Schwaighofer, S. Bernet, and M. Ritsch-Marte, "Near-perfect hologram reconstruction with a spatial light modulator," Opt. Express **16**(4), 2597 (2008).
33. P. Kunwar, L. Turquet, J. Hassinen, R. H. A. Ras, J. Toivonen, and G. Bautista, "Holographic patterning of fluorescent microstructures comprising silver nanoclusters," Opt. Mater. Express **6**(3), 946 (2016).